AX-PET: Concept, Proof of Principle and First Results with Phantoms

P. Beltrame, E. Bolle, A. Braem, C. Casella, E. Chesi, N. Clinthorne, R. De Leo, G. Dissertori, L. Djambazov, V. Fanti, C. Joram, H. Kagan, W. Lustermann, F. Meddi, E. Nappi, F. Nessi-Tedaldi, J. F. Oliver, F. Pauss, M. Rafecas, D. Renker, A. Rudge, U. Ruotsalainen, D. Schinzel, T. Schneider, J. Séguinot, P. Solevi, S. Stapnes, U. Tuna and P. Weilhammer

AX-PET Collaboration

***Abstract*—AX-PET is a novel PET concept based on long crystals axially arranged and orthogonal Wavelength shifter (WLS) strips, both individually readout by Geiger-mode Avalanche Photo Diodes (G-APD). Its design was conceived in order to reduce the parallax error and simultaneously improve spatial resolution and sensitivity. The assessment of the AX-PET concept and potential was carried out through a set of measurements comprising individual module characterizations and scans in coincidence mode of point-like and extended sources. The estimated energy and spatial resolutions from point-like measurements are R_{FWHM}=11.6% (at 511 keV) and 1.7-1.9 mm (FWHM) respectively as measured with point-like sources placed in different positions of the FOV. First results from scans of extended phantoms confirmed our expectations.**

I. Introduction

SPATIAL resolution and sensitivity are of major importance in determining the performances of PET scanners. We developed a PET demonstrator set-up based on axially oriented crystals whose axial coordinate can be retrieved by a hodoscope of Wavelength Shifter (WLS) strips interleaved with the LYSO crystal layers [1]. Both WLS strips and LYSO crystals are read out by Geiger-mode Avalanche Photodiodes (G-APD, also known as SiPM, MPPC) which are becoming the detector of choice in new PET developments given their insensitivity to magnetic fields and the large interest in PET/MRI combined imaging modality [2]. The innovative design of AX-PET decouples the spatial resolution and the sensitivity, allowing optimization of both at the same time. The AX-PET demonstrator set-up consists of two identical modules, which after a detailed individual characterization were set in coincidence to acquire various sources of increasing complexity. The system performance was evaluated against ^{22}Na point-like sources of rather low activity and complex extended phantoms filled with high concentrations of ^{18}F solution. The sources were placed on a rotary table to emulating a full scanner acquisition. A complete Monte Carlo model and reconstruction software, suited to the particular geometry of AX-PET, have been developed [3].

This work is partially supported by the Marie Curie ITN MC-PAD and the Intra-European Fellowship grant 237620 for the project INSPET.

P. Beltrame, A. Braem, C. Joram and T. Schneider are with CERN, PH Department, CH-1211 Geneva, Switzerland.

E. Chesi, H. Kagan, A. Rudge, J. Séguinot and P. Weilhammer are with Ohio State University, Columbus, Ohio 43210 USA.

C. Casella, G. Dissertori, L. Djambazov, W. Lustermann, F. Nessi-Tedaldi, F. Pauss, D. Renker and D. Schinzel are with ETH Zurich, CH-8092 Zurich, Switzerland.

D. Renker is currently with Technical University München, D-80333 München, Germany.

J. F. Oliver, M. Rafecas and P. Solevi are with IFIC (CSIC/Universidad de Valencia), E-46071 Valencia, Spain.

R. De Leo and E. Nappi are with INFN, Sezione di Bari, I-70122 Bari, Italy.

N. Clinthorne is with University of Michigan, Ann Arbor, MI 48109, USA.

E. Bolle and S. Stapnes are with University of Oslo, NO-0317 Oslo, Norway.

F. Meddi is with University of Rome "Sapienza", I-00185 Rome, Italy.

V. Fanti is with University of Cagliari and INFN, I-09124 Cagliari, Italy.

U. Ruotsalainen and U. Tuna are with Tampere University of Technology, FI-33100 Tampere, Finland.

Corresponding author e-mail: paola.solevi@cern.ch

II. The AX-PET concept

The main feature of AX-PET is axial orientation of the scintillation crystals (see Fig. 1) instead of a radial one, as in most PET scanners. The crystals are arranged in 6 layers of arrays of 8 crystals per layer. Each LYSO crystal is individually readout by a G-APD providing the transaxial coordinates (x,y) of the gamma interaction point and the deposited energy. In order to locate the gamma interaction in the axial direction i.e. z, the crystal layers are interleaved by arrays of 26 WLS strips each, also individually readout by G-APDs. As shown in Fig. 2, the scintillation light produced by the gamma interaction in LYSO is emitted isotropically. Part of the light is trapped within the crystal and collected by the photo-detector placed at one end of the scintillator bar. In order to enchance the light collection the LYSO surfaces are polished and the end face opposite to the one readout is coated with an Aluminium film. On the other hand a fraction of the light escaping the crystal is absorbed by the WLS strips and, after conversion toward longer wavelengths, is detected by the G-APDs. The strips which are fired in the event contribute to the computation of the z coordinate by a Centre Of Gravity (COG) method. The amount of light detected by each strip guarantees the z reconstruction capability down to an energy of at least 200 keV. The AX-PET design leads to a 3D reconstruction of the gamma interaction point with parallax free resolution. The segmentation of the detection volume enhances the amount of trackable Compton interactions whose interaction history can be properly reconstructed given the high spatial and energy resolutions (see Sec. IV). The use of properly reconstructed Compton events should allow to further enhance the sensitivity of the device, without resolution loss in the final image.

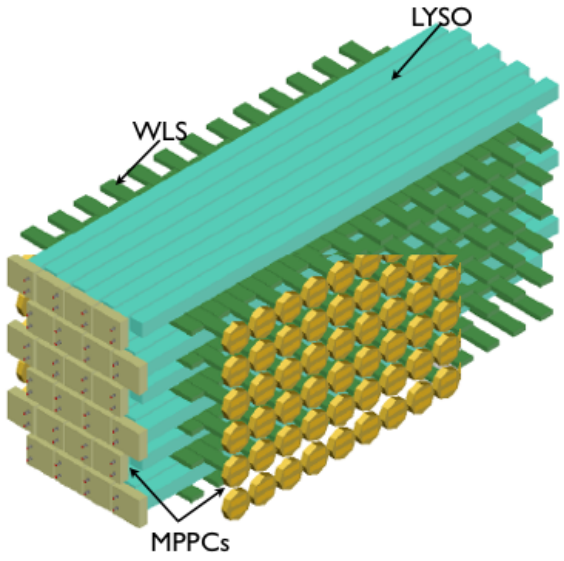

Fig. 1. A module of the AX-PET demonstrator with 8×6 LYSO crystals, axially oriented and orthogonally interleaved with WLS strips.

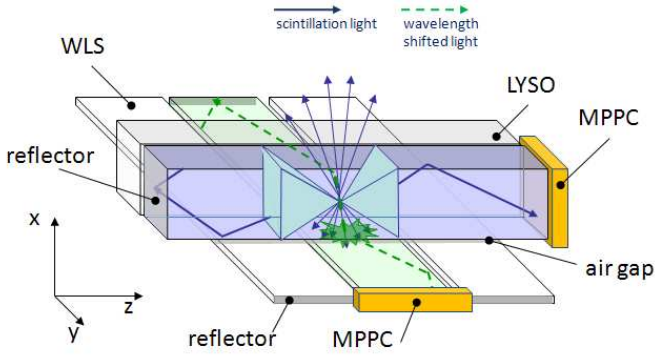

Fig. 2. AX-PET gamma detection and reconstruction principle.

III. The AX-PET module description

As described in the previous Section, one AX-PET module comprises 48 LYSO crystals and 156 WLS strips, arranged in a fully modular structure which allows easy replacement of components (in case of failure) [4]. A module is housed by an Aluminium structure. Special care was dedicated to the optimization of the components placement in order to minimize the gaps between crystals and guarantee an homogeneous sampling of the FOV.

Main components

The scintillation crystals are LYSO PreLude^{TM}420, manufactured by Saint-Gobain[1]. The crystals have the dimensions 3×3×100 mm^3. The crystals delivered by Saint-Gobain have been characterized in a dedicated set-up in terms of their intrinsic energy resolution and the effective optical absorption length. The average values $\Delta E/E_{intr}$ = 8.2±0.5% (FWHM) and λ_{eff} = 41.2±3.1 cm were obtained. LYSO crystals present a certain amount of natural activity (300 cps/cm^3) coming from the decay of ^{176}Lu, a natural beta emitter decaying in ^{176}Hf which de-excites by a 3 gammas cascade of 88, 202 and 307 keV.

The Wavelength Shifter (WLS) strips are EJ-280-10x produced by Ejien Technology[2]. They are Polyvinyltoluene strips of 3×0.9×40 mm^3 with high dye concentration leading to 0.4 mm absorption length at 425 nm. The absorbed light is isotropically re-emitted in the range 470-550 nm.

Both LYSO and WLSs are readout by G-APDs from Hamamatsu[3] (marketed as MPPC: Multi Pixel Photon Counter). The MPPCs of the LYSO are 3×3 mm^3, matching exactly the crystal cross section, divided into 3600 cells in order to match the expected number of optical photons collected. The MPPCs for the WLS strips are custom made with active area of 3.22×1.19 mm^3 divided into 782 cells. The MPPCs were attached by means of an optically transparent silicone glue to the WLS strips and crystals.

The response (i.e. gain) of the MPPCs is temperature dependent with a slope $dG/dT = -5\%/K$. In order to keep the system response stable, the temperature is monitored by four temperature sensors placed on the module frame. The bias voltage supplied to each MPPC is set with a precision of 7 mV according to the recorded temperature value. Variations of the temperature during the measurements are corrected offline during the data analysis.

The electronics chain of AX-PET consists at the front-end of fast amplifiers (Texas Instruments OPA843 for LYSO and OPA847 for WLS) which are fed with the MPPC signals via Kapton cables. The amplified signal has to pass a chosen threshold in order to be eventually readout. This threshold (LL) is set to 50 keV for LYSO crystals. The coincidences are formed between two modules when the sum of discriminated LYSO signals in both modules is in the range 400 keV (HL) and 600 keV (HHL). This ensures a good suppression of random coincidences as well as of scattered events. Additionally to the external modality, also an internal trigger option is available for testing and calibration purposes (i.e. any of the channels above threshold would start the aquisition).

IV. Measurements with point-like sources

The two AX-PET modules have been first fully characterized in a dedicated set-up built at CERN by using a point-like ^{22}Na source of about 600 kBq activity. The uniformity of the response of the detector has been measured and the energy calibrated, by correcting for the small deviation from linearity introduced by G-APD saturation. The final calibrated energy spectra (see Fig. 3) provide an average energy resolution of 11.7% FWHM at 511 keV over all the 96 LYSO crystals of the two modules.

For the study of the spatial resolution, the two modules were set in coincidence at a distance of 150 mm and the ^{22}Na point-like source placed at different positions of the FOV on a rotary table (see Fig. 4) .

In the transaxial plane (x,y) the resolution is driven by the size of the crystals i.e. 3×3 mm^2 cross-section yielding

[1]Saint-Gobain Cristaux, 77794 Nemours, France

[2]Eljen Technology, Sweetwater Texas 79556, United States

[3]Hamamatsu Photonics K.K., Japan

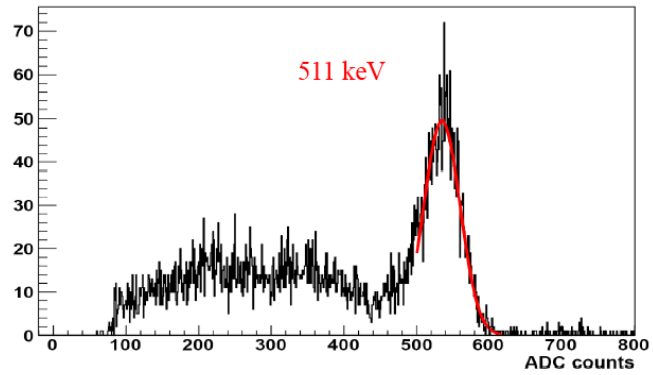

Fig. 3. Energy spectrum measured with a point-like ^{22}Na source.

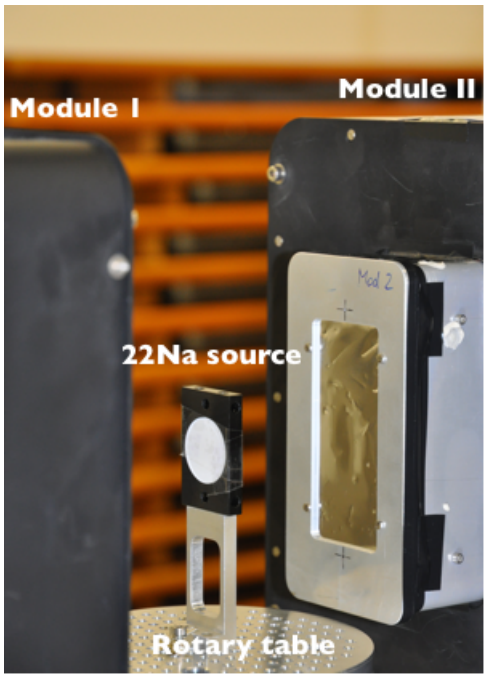

Fig. 4. Two modules of AX-PET are set in coincidence at a face-to-face distance of 150 mm. A ^{22}Na point-like source is placed in a plastic holder fixed to a rotary table and located at different position of the FOV.

$\sigma_{x,y}$ = 0.87 mm. In the axial direction the final resolution achieved is σ_z = 0.64 mm, once the contribution coming from the positron range and the source finite size is subtracted. The measurements with point-like sources aim as well at exploring the events "morphology" e.g. the number of hit LYSO (N_{LYSO}) in order to quantify the amount of Inter-Crystal Scatter (ICS) candidates to increase the sensitivity. The fraction of 1-LYSO events is ∼75%, the remaining part is mostly coming from 2-LYSO hit events (see Fig. 5).

A set of tomographic reconstructions was carried out with ^{22}Na sources in different positions of the FOV. The rotary table was moved in steps of 10 degrees. To reconstruct the images, a dedicated reconstruction algorithm, based on Maximum-Likelihood Expectation Maximization (MLEM) was employed. The System Matrix (SM) was computed using multi ray-tracing techniques. It models in details the special geometry of the system and takes into account crystal attenuation and penetration effects (inner layers screen outer layers). Each acquired data set was processed in order to select good events with only 1-LYSO hit per module. The spatial resolution obtained in all 3 dimensions is in the range 1.7-1.9 mm (FWHM) (see Fig. 6).

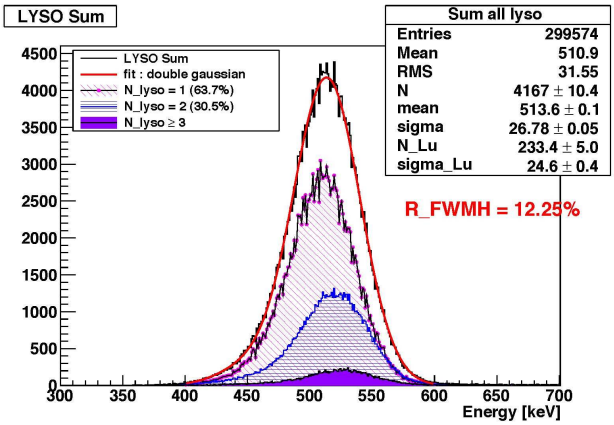

Fig. 5. Summed energy spectra of the LYSO crystals at different crystal multiplicities (N_{LYSO} = 1,2,3 or more). The percentage of events with 1 and 2 hit crystals are, respectively, 75% and 25%

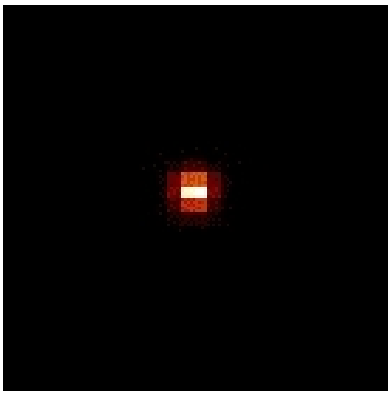

Fig. 6. Image in the transaxial plane of a reconstructed point-like source in the middle of the FOV. The voxel size in the reconstruction is 0.7×0.7×0.7 mm^3. The source has been reconstructed by using a dedicated MLEM algorithm with 30 iterations.

V. Measurements of Extended Sources

The AX-PET prototype has been recently tested (April 2010) at the Radiopharmaceutical laboratory at ETH Zurich (Switzerland) by measuring different phantoms, fitting the size of the FOV (30×30×80 mm^3), constrained by having only two modules with a rotating source[4]. To assess the resolution of the scanner, a set of thin 3 cm long capillaries (see Fig. 7) and micro-Derenzo phantoms were employed. To further investigate the image quality, a mouse-like phantom homogeneously filled with radioactive solution was measured. All phantoms were filled with various concentrations of ^{18}F. As with the point-like source, the acquisition was performed by rotating the source over π in steps of 10 degrees. The

[4]In the meantime also measurements with an extended field of view were performed, in which one AX-PET module was rotated with respect to the 180° position

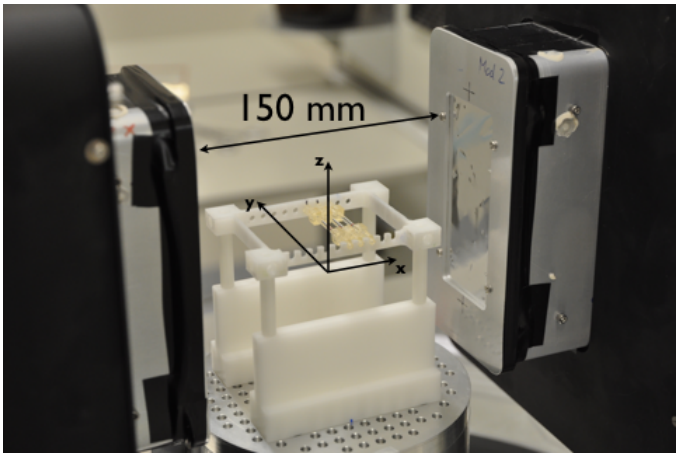

Fig. 7. Picture of the two modules in the measurements set-up at the ETH radiopharmaceutical lab. The 3 capillaries are placed on a source holder fixed to a rotary table.

capillaries have been located in the FOV in different planes i.e. parallel to x, y and z. As an example, the results of the reconstructed images of three capillaries placed with a 4.5 mm pitch in y are presented in Fig. 8. The other 2 sets of capillaries have been also reconstructed and analyzed. The FWHM has been estimated by a Gaussian fit for each capillary in the 3 data sets in order to estimate the dependence of the resolution on the position in the FOV. The prototype presents a homogeneous resolution in the 3 dimensions with an average value $\sim$2.0 mm (FWHM) which still includes the contribution of the finite size of the capillary (1.4 mm inner diameter).

VI. Conclusions

The tests carried out with point-like sources and extended phantoms confirmed the expected resolution of at least 2.0 mm (FWHM) in all three dimensions and also the photon tracking capability of the device. More performance aspects will be assessed in a second measurement campaign with a new set-up comprising the possibility to change the relative angle between the two modules, allowing to scan a larger FOV. The analysis of the available data showed that an improved understanding of the count loss phenomena, related to the prototype front-end electronics and DAQ system, will allow achieving a superior image quality. The reconstruction still needs to be improved before any final performance assessment of AX-PET can be done. An analytical reconstruction algorithm based on Filtered Back Projection (FBP) is under development and will be used for a better assessment.

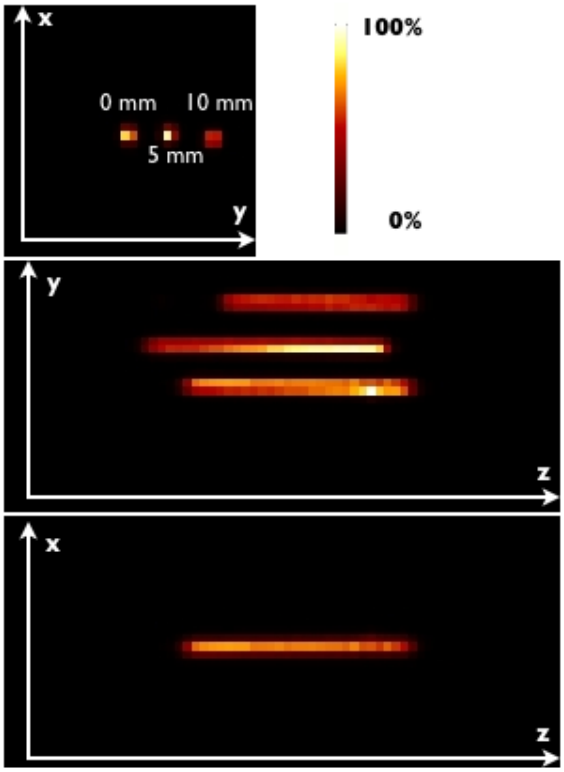

Fig. 8. Images of the three reconstructed capillaries (see Fig.7) in the transverse (top), sagittal (centre) and coronal (bottom) planes, in hot metal scale (voxel size is $1\times1\times1$ mm^3).

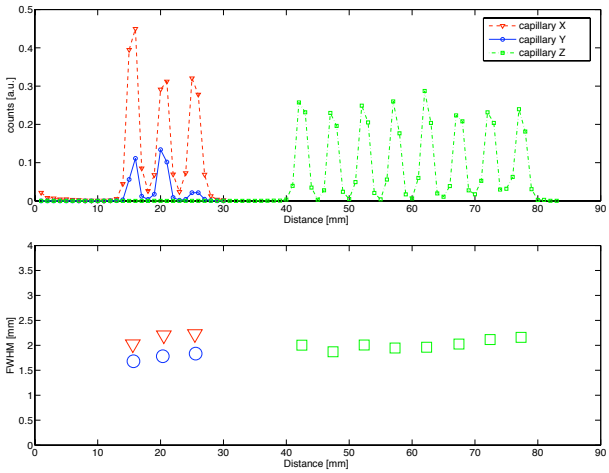

Fig. 9. Spatial resolution (FWHM) for the capillary measurements in different positions of the FOV. The SM voxel size is 1 mm^3 and the plotted resolution still includes the size of the capillaries (1.4 mm inner diameter).

Acknowledgment

The authors would like to thank our technical staff for its competent support of this activity. We are indebted to the team of S. M. Ametamey and Dr. S. Krämer from the Animal PET lab ETH Zurich (Switzerland) and A. Hohn from PSI for their support of our measurement campaign at the ETH Zurich.

References

[1] A. Braem et al., *AX-PET: A novel PET detector concept with full 3D reconstruction*, Nucl. Instr. Meth. A 610 (2009) 192-195.
[2] A.W. Sauter, H.F. Wehrl, A. Kolb, M.S. Judenhofer, B.J. Pichler, *Combined PET/MRI: one step further in multimodality imaging*, Trends Mol Med. 2010 Nov, 16(11), 508-15.
[3] A. Braem et al., to be submitted to Phys. Med. Biol.
[4] A. Braem et al., to be submitted to Nucl. Instr. Meth. A.